15 Aug 2008, 11:00am - 12:30pm

Structural Response of FRP Reinforced Concrete Softeyes for Tunnel Excavation

Fabio Matta
University of Miam, iCoral Gables, Florida

Antonio Nanni
University of Miami, Coral Gables, Florida


6th International Conference on
Case Histories in Geotechnical Engineering, Arlington, VA, August 11-16, 2008

STRUCTURAL RESPONSE OF FRP REINFORCED CONCRETE SOFTEYES FOR TUNNEL EXCAVATION

Fabio Matta
University of Miami
Coral Gables, Florida-USA 33146

Antonio Nanni
University of Miami
Coral Gables, Florida-USA 33146

ABSTRACT

The development of pultruded glass fiber reinforced polymer (GFRP) bars for internal reinforcement of concrete, together with dedicated limit-state design guidelines, has led to a recent breakthrough in the field of tunnel excavation. The use of GFRP bars in softeyes, which are openings of retaining walls to be penetrated by tunnel boring machines (TBMs) during excavation, is becoming mainstream. The low shear strength and brittleness compared to steel bars facilitate and expedite excavation, resulting in time and cost saving, as well as improved safety. Large-size (#10) GFRP bars are typically used as flexural reinforcement for the massive softeyes, often in bundles. However, the flexural and shear design algorithms adopted by the American Concrete Institute (ACI) for fiber reinforced polymer (FRP) reinforced concrete (RC) have never been experimentally validated with full-scale tests. Question marks exist on potential detrimental effects on the concrete shear strength contribution that accrue from size effect, and on the flexural strength of RC members due to shear lag in the large-size longitudinal reinforcement, and due to the use of bar bundles. In this paper, the fundamentals of flexural and shear design of FRP RC are first outlined. Then, an experimental program that included bending tests on five full-scale softeye beam specimens is presented and discussed. The test matrix was designed to study the shear and flexural response of large-scale members using different layouts of flexural and shear reinforcement. The results demonstrate the validity of the current ACI design algorithms, and back the identification of areas of research to improve their efficiency.

INTRODUCTION

The peculiar properties of glass fiber reinforced polymer (GFRP) bars for internal reinforcement of structural concrete lend themselves to relevant geotechnical applications. For instance, the superior corrosion resistance compared to steel make GFRP bars suitable for use in retaining walls in highly corrosive environments, such as coastal bluffs (Fig.1). A major breakthrough lies, however, in the use to construct "softeye" openings in temporary retaining walls for tunnel excavation. The softeyes are the sections of either cast-in-place diaphragm or bore-pile reinforced concrete (RC) walls to be penetrated by the tunnel boring machine (TBM). The walls are typically part of the RC shafts used to launch and to recover the TBM at commencement and termination of the excavation, respectively. Only a few TBMs are specifically designed to cut through steel RC walls, where the steel bars prevent propagation of the cracks in the mass concrete, and further resist progression of the disc cutters by undergoing plastic deformation instead of fracturing. Hydraulic breaking and cutting equipment was typically used to break through the RC walls and allow the TBM to either access or being recovered. The low shear strength and brittleness of pultruded GFRP bars are highly desirable properties in such instance. Penetration of conventional TBMs becomes feasible without preliminary breaking of the RC walls (Fig. 2), thereby expediting the field operations, and resulting in substantial time and cost saving, as well as improved job site safety. In addition, the light weight of GFRP bars (about one quarter that of steel) simplifies construction and handling of the reinforcement cages. The technology has been first deployed in early 2000 for the excavation of the Kwai Shing Tunnel in Hong Kong, PRC, and has since been successfully implemented in several projects in Asia, Europe, and North America (Mielenz 2003, Nelson 2006, Schürch and Jost 2006, Thasnanipan *et al.* 2000).

Large-size GFRP bars (#10, *i.e.*, with nominal diameter of 1.25") are normally used as tensile reinforcement for the massive softeyes, often in bundles (Fig. 3). Design principles are well established, and substantially differ from those of steel RC (Bank 2006, Nanni 1993, 2003). Guideline documents have been published in North America, Europe, and Japan. In the USA, the reference document is the "Guide for the Design and Construction of Structural Concrete Reinforced with FRP Bars – ACI 440.1R-06" by the American Concrete Institute (ACI 440 2006). The guidelines improve the 2001 and 2003 versions by reflecting the knowledge gained through extensive theoretical and experimental research that was performed in recent years. However, the algorithms used for the flexural and shear design of GFRP RC structures have never been validated on members with large sizes that are, in fact, typical of softeye designs.

(a)

(b)

Fig. 1. Use of GFRP bars in retaining wall in coastal bluff: site (a), and reinforcement cage (b). Credit: Hughes Brothers.

(a)

(b)

Fig. 2. Use of GFRP bars in softeye: installation of wall reinforcement (a), and TBM breakthrough (b). Credit: Hughes Brothers (a), and Jacobs Engineering Group (b).

(a)

(b)

Fig. 3. GFRP #10 bars: closeup (a), and softeye cage under construction (b). Credit: Hughes Brothers (b).

In this paper, the fundamentals of flexural and shear design of structural concrete reinforced with fiber reinforced polymer (FRP) bars are first outlined. Then, an experimental program that included four-point bending tests on five full-scale softeye beam specimens is presented and discussed. The test matrix was designed to: a) study the shear and flexural response of large-scale members using different layouts of flexural and shear reinforcement; and b) address concerns on potential detrimental effects on the concrete shear strength due to size effect (Bažant and Kim 1984, Collins and Kuchma 1999, Kani 1967), and on the flexural strength due to shear lag in the large-size longitudinal reinforcement (*i.e.*, non uniform stress distribution in the bar cross section), and due to the use of bundles of large-size (#10) bars. From a practical standpoint, the objective was to provide experimental evidence to assess the validity of the current ACI design algorithms (ACI 440 2006) for the design of softeyes.

ACI 440 DESIGN PROVISIONS

The design principles for FRP RC reflect the different philosophy with respect to traditional steel RC design, which stems from the peculiar physical and mechanical properties of FRP materials. The most relevant are the brittle behavior in tension in the fiber (axial) direction, the smaller axial stiffness than steel (the elastic modulus of unidirectional GFRP in the fibers direction, E_f, is typically around 6 msi); and the reduced

transverse strength and stiffness of the bars, where the properties are dominated by those of the polymeric matrix. Following, the salient aspects of the limit-state ACI 440 flexural and shear design methodologies (ACI 440 2006) are summarized.

Flexure

The nominal flexural strength of FRP RC members, M_n, is computed in a straightforward manner based on strain compatibility, internal force equilibrium, and the controlling mode of failure. Plane sections are assumed, together with perfect bond between the FRP bars and the surrounding concrete, zero tensile strength of the concrete, and limiting concrete compression strain of 0.003 (which entails use of the equivalent ACI rectangular stress block). Since FRP bars exhibit a linear elastic behavior up to failure, tension-controlled designs would produce RC members that fail in a brittle (catastrophic) manner. Limited warning of impending failure would only be given by extensive cracking and large deflection, as produced by the significant elongation of the reinforcing bars due to their relatively small axial stiffness. Some inelastic behavior is displayed when crushing of the concrete is the governing failure mode, thus making over-reinforced sections marginally more desirable (Nanni 1993). The lack of ductility is compensated in the computation of the design flexural strength, ϕM_n, by applying a reduction factor of $\phi = 0.55$ for tension-controlled members, compared to 0.90 of steel RC, which linearly increases to a maximum of 0.65 for compression-controlled members where the reinforcement ratio is equal or greater than 1.4 times the balanced value (*i.e.*, $\rho_f \geq 1.4\ \rho_{fb}$).

Serviceability is evaluated on the basis of maximum crack width and deflection, for which formulations are provided. The latter parameter is computed by using a modified Branson's equation for the effective moment of inertia of a cracked member, which is expressed as

$$I_e = \left(\frac{M_{cr}}{M_a}\right)^3 \beta_d I_g + \left[1 - \left(\frac{M_{cr}}{M_a}\right)^3\right] I_{cr} \leq I_g \qquad (1a)$$

where M_{cr} = cracking moment, M_a = applied moment, I_g = gross moment of inertia, I_{cr} = moment of inertia of the transformed cracked section, and

$$\beta_d = \frac{1}{5}\left(\frac{\rho_f}{\rho_{fb}}\right) \leq 1.0 \qquad (1b)$$

is the coefficient that accounts for reduced tension stiffening.

Shear

The nominal shear strength of an FRP RC cross section, V_n, is approximated as the sum of the shear resistance provided by the concrete, V_c, and by the shear reinforcement, V_f.

The smaller axial stiffness of FRP reinforcement compared with steel results in RC cross sections with deeper and wider cracks, and thus with smaller shear resistance provided by both aggregate interlock and compressed (uncracked) concrete. In addition, the low transverse strength and stiffness may reduce the strength contribution due to dowel action. The concrete shear strength is expressed in the form

$$V_c = 5\sqrt{f'_c}\, b_w c \qquad (2)$$

where f'_c = cylinder compressive strength of concrete, b_w = width of the web, and c = depth of the neutral axis.

The strength contribution of FRP vertical stirrups spaced on-center at a distance s, upon engagement once crossed by a diagonal crack, is computed following a common straightforward approach as

$$V_f = A_{fv} f_{fv} \frac{d}{s} \qquad (3a)$$

thus assuming formation of the failure crack at a 45° angle, where d = effective depth of the cross section, and where the stress in the shear reinforcement, f_{fv}, is limited as

$$f_{fv} = 0.004 E_f \leq f_{fb} \qquad (3b)$$

to control crack width, prevent degradation of aggregate interlock,, and avoid failure at the bent portion of the FRP stirrup, where the strength is f_{fb}. The shear strength reduction factor $\phi = 0.75$ applies to compute the design strength, ϕV_n.

EXPERIMENTAL STUDY

Specimens

The test matrix comprises five large-size, 30' long GFRP RC beams that were designed according to the ACI 440 guide (ACI 440 2006). Figure 3 shows the cross section and the flexural and shear reinforcement layout of Specimens 1, 2, 3A, 3B and 4. The overall height (38.5") and the effective depth of the cross sections were selected as representative of typical softeyes. The flexural reinforcement consisted of #10 GFRP bars. U-shaped #5 GFRP bars were arranged in the form of closed stirrups to provide shear reinforcement.

Table 1 summarizes the nominal and design flexural strength and the associated maximum shear force, $V(M_n)$, and the nominal and design shear strength of the specimens. The values are computed assuming nominal concrete strength of 4000 psi, #10 bar strength and longitudinal elastic modulus of 74.0 ksi and 5.90 msi, and #5 stirrup strength and modulus of 95.0 ksi (45.6 ksi at the bends) and 5.90 msi.

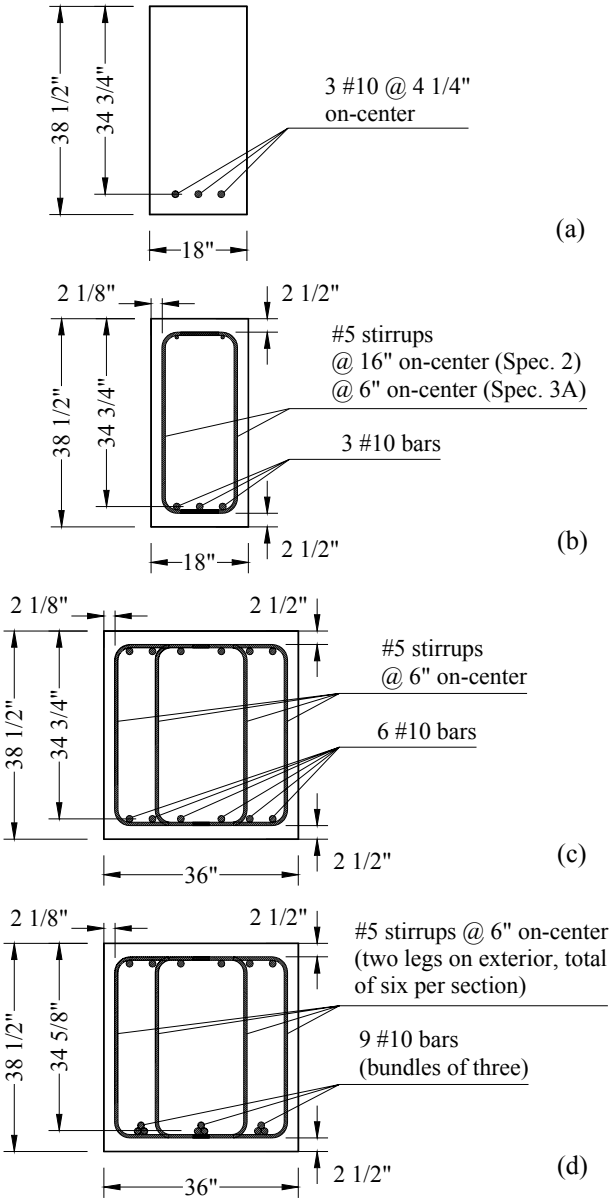

Fig. 3. Cross section of GFRP RC beam specimens: 1 (a), 2 and 3A (b), 3B (c), and 4 (d).

Table 1. Nominal and Design Strength per ACI 440 (2006)

Specimen	1	2	3A	3B	4
Flexure					
M_n (kip-ft)	754.9	754.9	754.9	1509.7	2235.3
$V(M_n)$ (kip)	83.9	83.9	83.9*	167.7*	248.4*
ϕM_n (kip-ft)	415.2	415.2	415.2	830.4	1327.4
Shear					
V_c (kip)	25.6	25.6	25.6	51.1	61.7
V_f (kip)	-	31.4	83.9	167.1	250.7
V_n (kip)	25.6*	57.1*	109.5	219.0	312.4
ϕV_n (kip)	19.2	42.8	82.1	164.2	234.3

* Governs failure. Self weight is neglected.

Three longitudinal bars were used as the sole reinforcement for Specimen 1 [Fig. 3(a)], in order to evaluate the concrete shear strength, V_c, and the impact of size effect. The resulting nominal GFRP reinforcement ratio $\rho_f = 0.59\%$ corresponds to an effective reinforcement ratio (*i.e.*, corrected by a factor E_f / E_s, where E_s = elastic modulus of steel, to account for the smaller FRP longitudinal elastic modulus, E_f) $\rho_{eff} = 0.12\%$. This value lies below the minimum $\rho_{eff} = 0.15\%$ used in experimental studies that have been reported in the literature, and which provided the results to calibrate Eq. (2) (Tureyen & Frosch 2003). Such ratio is still representative of lower-bound real-case scenarios, and was selected since size effect on the shear strength becomes more relevant at smaller reinforcement ratios.

The same flexural reinforcement layout was used in Specimens 2 and 3A [Fig. 3(b)], together with #5 stirrups spaced at a distance s = 16" (which is associated with the minimum shear reinforcement, as required in most structures, and is given by $s_{max} = A_{fv}f_{fv} / 50b_w$) and 6" on-center, respectively. Specimen 2 served to evaluate the ability of the shear reinforcement to provide required the post-cracking strength, V_f, up to shear failure at nominal 57.1 kip (Table 1). Conversely, the shear reinforcement of Specimen 3A was designed to have the flexural strength to govern failure, with rupture of the GFRP bars resulting from a longitudinal reinforcement ratio of 0.78 times the balanced value, at a nominal bending moment of 754.9 kip-ft (Table 1). Specimen 3B [Fig. 3(c)] is replicate of two 3A sections cast side-by-side and provides a valid counterpart to study the flexural response of Specimen 3A.

Specimen 4 [Fig. 3(d)] was designed to assess flexural strength when using bundles of longitudinal bars, as often encountered in practice. Bundles of three #10 bars were used, providing a nominal moment capacity of 2243.6 kip-ft (Table 1). Concrete crushing was expected to govern failure, due to the nominal longitudinal reinforcement ratio of 1.17 times the balanced value.

Materials

The reinforcement cages for the specimens were constructed with pultruded E-glass/vinyl ester GFRP #10 bars and #5 C-shaped bars to form the stirrups. Average tensile strength and elastic modulus of eight #10 bar samples were f_{fu} = 67.0 ksi and E_f = 5.90 msi for Specimens 1, 2 and 3A, and 67.4 ksi and 5.51 msi for Specimens 3B and 4. Average tensile strength and elastic modulus of six #5 stirrup samples were 100.1 ksi and 5.83 msi. The beams were cast using normal weight concrete. Average cylinder compressive strength was determined per ASTM C 39 as f'_c = 4276 psi, 5627 psi, 5134 psi, 4206 psi and 4569 psi for Specimens 1, 2, 3A, 3B and 4, respectively, at the time of testing.

Test Setup

The beams were tested in four-point bending using the setup illustrated in Fig. 4 (Specimens 1, 2 and 3A) and Fig. 5 (Specimens 3B and 4). The latter was implemented to facilitate detection and observation of the flexural cracks, and to simplify inspection of the longitudinal reinforcement in the failed specimens. A shear span of 9' provided a shear span to effective depth ratio of 3.1, which was aimed at obtaining a lower-bound

value for V_c. The constant moment region was 6'. An anchorage length of 3' was provided past the end supports to prevent bar slip.

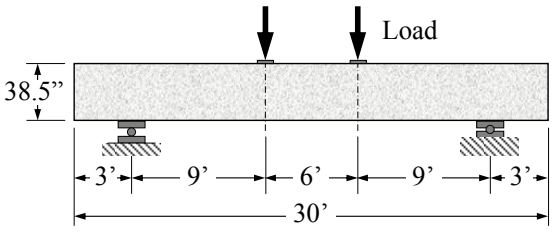

(a)

(b)

Fig. 4. Test setup for Specimens 1, 2 and 3A: schematic (a), and photograph (b).

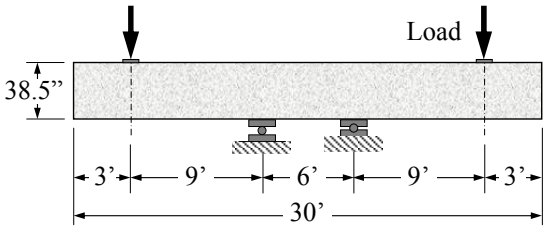

(a)

(b)

Fig. 5. Test setup for Specimens 3B and 4: schematic (a), and photograph (b).

The simple support and the hinged support were simulated by means of assemblies including steel cylinders that were sandwiched between two flat and grooved steel plates, respectively. Plywood sheets with thickness of 0.25" were inserted between the steel plate and the concrete surface at the supports and at the loading sections. The loads were applied via manually operated hydraulic jacks with 400 kip capacity, and were measured at each loading section with an 200 kip capacity load cell.

The specimens were extensively instrumented with strain gauges to measure strain in the GFRP reinforcement and in the concrete at selected relevant sections and locations. Direct Current Linear Variable Differential Transformer (DC-LVDT) and draw-wire transducers were used to measure deflections along the length of the beams.

RESULTS AND DISCUSSION

Figures 6 and 7 show the experimental load-displacement response of Specimens 1, 2 and 3A, and of Specimens 3A and 4, respectively. The load reported in the graphs is measured at either loading section. Displacement is measured at the mid-section of the first three beams, which were tested using the setup in Fig. 4, and at either loading section of Specimens 3B and 4, which were tested using the setup in Fig. 5.

Dashed lines indicate the load level associated with the nominal strength (either shear, V_n, or flexural, M_n) and design strength (either ϕV_n or ϕM_n), which were computed using the experimental material properties of concrete, and GFRP bars and stirrups. The effect of self weight is accounted for. The results are presented and discussed as follows on the basis of strength and deflection (stiffness) response.

Strength

Shear failure of Specimen 1, which had no shear reinforcement, occurred at a load of 30.5 kip, thus well above the nominal value of 19.7 kip [Fig. 6(a)].

The likely relevance of the role of size effect is illustrated in Fig. 8, where the ratio between the experimental and the theoretical concrete shear strength, ($V_{c,experimental}$ / $V_{c,ACI\ 440}$), is plotted against the effective reinforcement ratio and the effective depth for Specimen 1 and other 52 FRP RC beams found in the literature (Matta *et al.* 2007). The ratio for Specimen 1 is 1.41, thus pointing out a good safety margin. However, such value is about 30% smaller than the average for similar reinforcement ratios in the literature [Fig. 8(a)], where the tests were performed on beams without shear reinforcement and with effective depth d = 6.2". Figure 8(b) shows that higher ratios of experimental versus theoretical concrete shear strength were typically reported in the literature for FRP RC beams having effective depths d ≤ 14.8" (thus much smaller than Specimen 1), irrespectively of the amount of reinforcement. A photograph of the beam after failure is shown in Fig. 9(a).

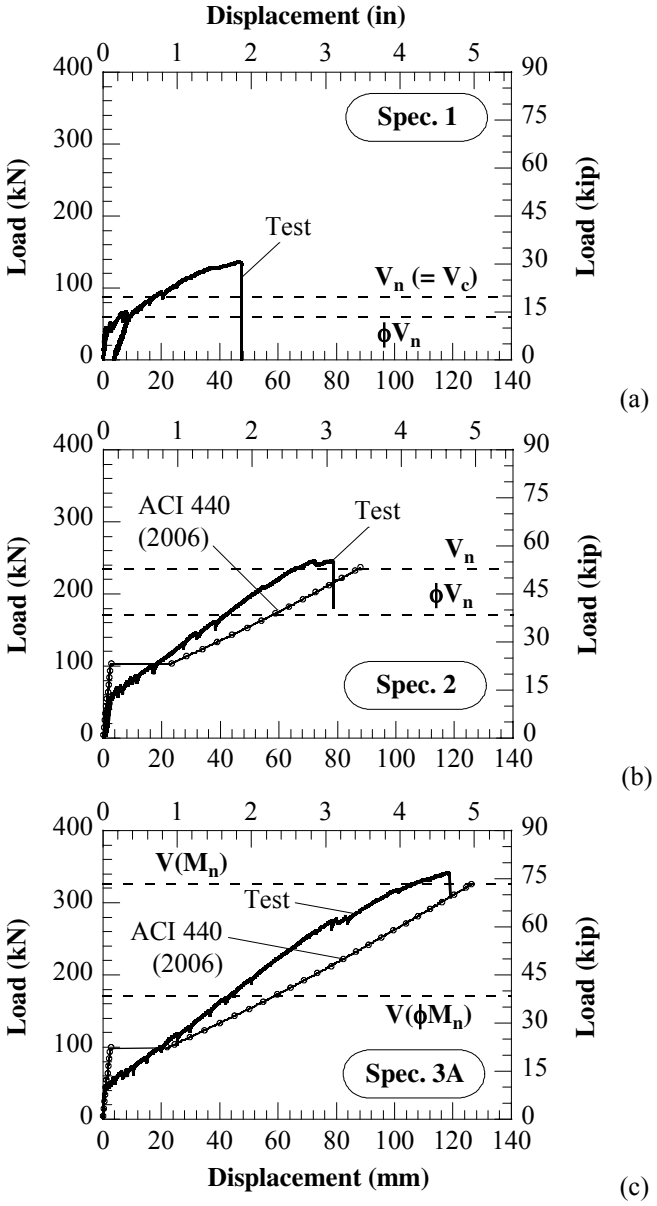

Fig. 6. Experimental and analytical load-displacement response of Specimens 1 (a), 2 (b), and 3A (c).

The use of the required minimum shear reinforcement allowed Specimen 2 to attain a maximum load of 55.2 kip, as the primary shear crack propagated deep into the compression zone [Figs. 6(b) and 9(b)]. This load is slightly greater than the nominal value of 52.8 kip, and well above the design limit of 38.0 kip. Specimen 3A was designed to fail in flexure, providing additional strength compared to Specimen 2 by decreasing the stirrup spacing from 16" to 6". A maximum load of 76.7 kip was reached [Fig. 6(c)], as rupture of the three #10 longitudinal bars occurred at 12" outwards from the nearby loading section [Figs. 9(c) and 10(a)]. The test result exceeds the 73.2 kip load associated with the nominal strength, and was largely above the design value of 37.9 kip, due to the 0.55 strength reduction factor applied to compute the design moment capacity of under-reinforced FRP RC sections (ACI 440 2006).

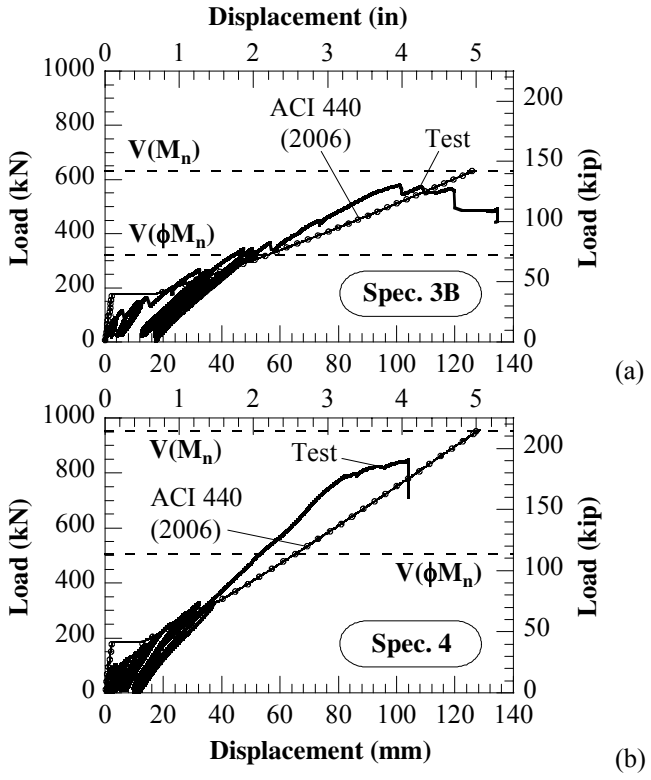

Fig. 7. Experimental and analytical load-displacement response of Specimens 3B (a) and 4 (b).

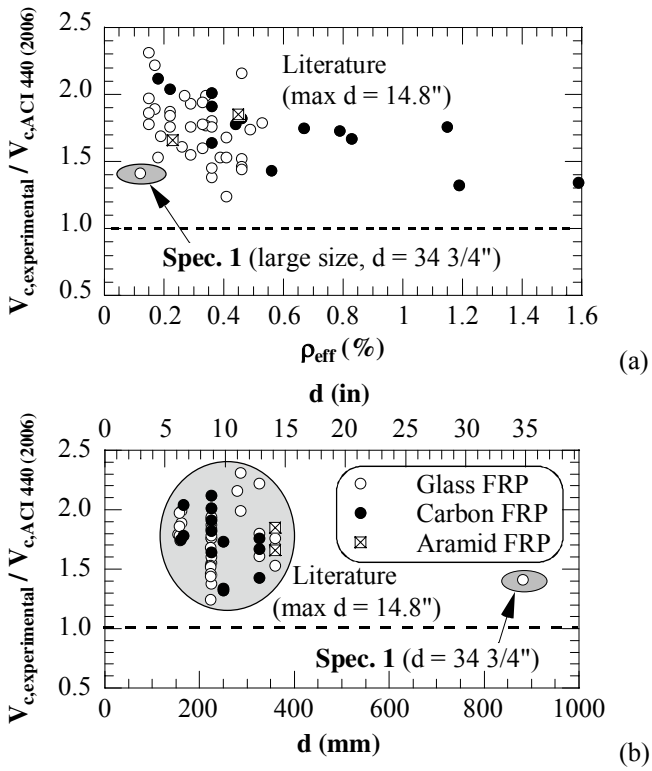

Fig. 8. Ratio of experimental to theoretical concrete shear strength in FRP RC beams without shear reinforcement with respect to: effective reinforcement ratio (a) and depth (b).

(a)


(b)

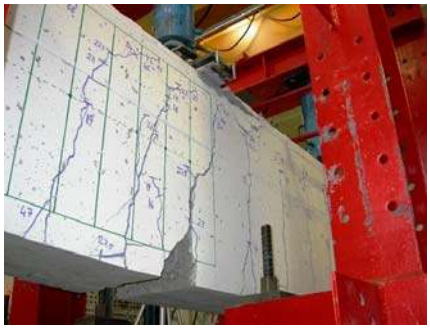
(c)


(d)


(e)

Fig. 9. Photos of beam specimens after failure: 1 (a), 2 (b), 3A (c), 3B (d) and 4 (e).


(a)

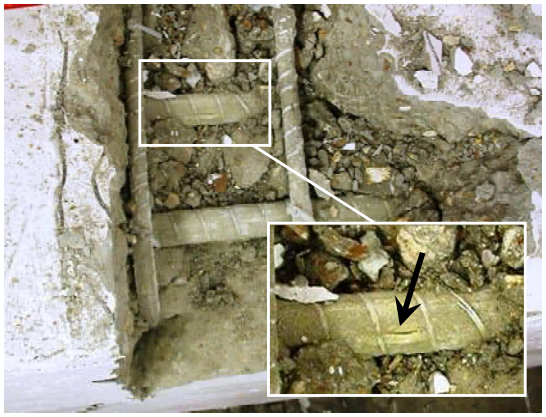
(b)

(c)

Fig. 10. Photos of longitudinal #10 GFRP bars at failure section in Specimens 3A (a), 3B (b) and 4 (c).

However, the parent Specimen 3B (replicate of two Specimens 3A side-by-side) failed in shear compression at a load of 129.6 kip, slightly below its nominal strength in flexure at 141.9 kip [Fig. 7(a) and 9(d)]. In fact, inspection of the reinforcement at the failure section revealed some delamination on the GFRP bars [Fig. 10(b)], which stands as a clear sign of impending rupture. While Specimens 3A and 3B largely exceeded their design strength, the difference in failure mode calls for further investigation on the effectiveness of FRP shear reinforcement in providing the strength contribution, V_f, assumed in design.

Specimen 4 reached its moment capacity at a load of 190.6 kip,

again fairly close to the level of 215.5 kip associated with the nominal flexural strength, and well above the 113.5 kip mark associated with the design flexural strength [Fig. 7(b)]. The failure mode was rupture of the longitudinal bars [Fig. 9(e) and Fig. 10(c)]. This was consistent with the actual GFRP reinforcement ratio, ρ_f = 0.89%, of 0.91 times the value of balanced failure, ρ_{fb} = 0.98%, as computed using the material properties determined experimentally. The results for Specimen 4 are positive, since rupture of the bundled bars was attained. Further research is needed to characterize the influence on the response of FRP RC members, if any, of using bar bundles as longitudinal reinforcement, especially in the case of larger bundles than in the present investigation.

Deflection

The theoretical approximations of the load-deflection response of Specimens 1, 2 and 3A, and of Specimens 3B and 4, are shown together with the experimental results in Fig. 6 and Fig. 7, respectively. The deflection is computed by approximating the flexural stiffness as E_cI_e, where E_c is the concrete elastic modulus, and I_e is the effective moment of inertia. I_e varies between the gross moment of inertia, I_g, and the moment of inertia of the transformed cracked section, I_{cr}, and is determined as a function of the applied moment via Eq. 1(a). The reduced stiffness, which is typically displayed when using FRP reinforcement as compared to steel, is rendered in Eq. 1(a) by means of a reduction coefficient for tension stiffening, β_d, given by Eq. 1(b). This equation was introduced in the ACI 440 guidelines (ACI 440 2006) to replace the formulation for β_d in the 2003 guidelines, which produced unconservative results. An alternative approach that does not originate from Branson's and that produces valid results was also proposed (Bischoff 2007).

Comparison of the experimental and analytical curves shows that the ACI formulation (ACI 440 2006) yields results that are not over-conservative, and can be used for design purposes.

CONCLUSIONS

This paper reports on the first experimental program aimed at evaluating the strength of large-size GFRP RC beams representative of full-scale softeye wall strips, and assess the effectiveness of the current ACI design algorithms (ACI 440 2006). The reinforcement layout of the beam specimens was designed to have failure controlled by shear (Specimens 1 and 2) and flexure (Specimens 3A, 3B and 4). The following conclusions can be drawn:

1) All specimens failed at loads that clearly exceeded the design strength associated with the governing failure mode. The margin ranged between a minimum of 45.3% and maximum of 102.4% for Specimens 2 and 3A, respectively. The results substantiate the ACI design algorithms for the flexural and shear design of large-size FRP RC members, such as in the case of GFRP RC softeyes.

2) The concrete shear strength, V_c, appears to be strongly affected by size effect. A strength reduction of about 30% was noted for Specimen 1 with respect to scaled counterparts without shear reinforcement reported in the literature, in agreement with a previous study (Matta *et al.* 2007). However, the conservativeness of the design algorithm for V_c (ACI 440 2006, Tureyen and Frosch 2003) contributes to offset the size effect (Matta *et al.* 2007).

3) Further research is needed to study: the extent of size effect on the concrete shear strength in FRP RC beams; the effectiveness of FRP shear reinforcement in providing the strength contribution, V_f, assumed in design; and the limitations for the efficient use of bundles of bars for flexural reinforcement, particularly when large diameters are needed (*e.g.*, #10 bars), such as in the case of softeyes.

ACKNOWLEDGEMENTS

The financial support of the NSF I/UCRC "Repair of Buildings and Bridges with Composites" (RB^2C), and the assistance of the Center's industry member Hughes Brothers, Inc. in supplying the FRP reinforcement are gratefully acknowledged. The experimental tests reported herein were performed at the Structures Laboratory of the Missouri University of Science and Technology, and thanks are due to the following individuals for their assistance: Travis Hernandez and Jason Cox (lab technicians), Gary Abbott (electronic technician), Dr. Nestore Galati (formerly Research Engineer), Flavio Mosele (formerly Visiting Scholar from the University of Padova, Italy), and Preeti Shirgur (formerly Graduate Research Assistant).

REFERENCES

American Concrete Institute (ACI) Committee 440 [2006]. "*Guide for the Design and Construction of Structural Concrete Reinforced with FRP Bars – ACI 440.1R-06*". ACI, Farmington Hills, MI.

Bank, L.C. [2006]. "*Composites for Construction: Structural Design with FRP Materials*". John Wiley & Sons, Hoboken, NJ.

Bažant, Z.P. and J.-K. Kim [1984], "Size Effect in Shear Failure of Longitudinally Reinforced Beams," *ACI Journal*, Vol. 81, No. 5, pp. 456-468.

Bischoff, P.H. [2007]. "Deflection Calculation of FRP Reinforced Concrete Beams Based on Modifications to the Existing Branson Equation," *Journal of Composites for Construction*, Vol. 11, No. 1, pp. 4-14.

Collins, M.P. and D. Kuchma [1999], "How Safe Are Our Large, Lightly Reinforced Concrete Beams, Slabs, and Footings?," *ACI Structural Journal*, Vol. 96, No. 4, pp. 482-490.

Kani, G.N.J. [1967], "How Safe Are Our Large Reinforced Concrete Beams?," *ACI Journal*, Vol. 64, No. 3, pp. 128-141.

Matta, F., A. Nanni, N. Galati and F. Mosele [2007], "Size Effect on Shear Strength of Concrete Beams Reinforced with FRP Bars," *Proc. 6th Intern. Conf. on Fracture Mechanics of Concrete and Concrete Structures (FraMCoS-6)*, Catania, Italy, Taylor & Francis, pp. 1077-1084.

Mielenz, J. [2003], "Breakthrough Technology on CTRL," *Tunnels & Tunneling International*, Vol. 35, No. 4, pp. 24-26.

Nanni, A. [1993], "Flexural Behavior and Design of RC Members Using FRP Reinforcement," *Journal of Structural Engineering*, Vol. 119, No. 11, pp. 3344-3359.

Nanni, A. [2003], "North American Design Guidelines for Concrete Reinforcement and Strengthening Using FRP: Principles, Applications and Unresolved Issues," *Construction and Building Materials*, Vol. 17, No. 6-7, pp. 439-446.

Nelson, J. [2006], "Composite Rebar Speeds Tunneling Operations," *Composites Technology*, April Issue, pp. 44-46.

Schürch, M. and P. Jost [2006], "GFRP Soft-Eye for TBM Breakthrough: Possibilities with a Modern Construction Material," *Proc. Intern. Symposium on Underground Excavation and Tunnelling*, Bangkok, Thailand, 8 pp.

Thasnanipan, N., A.W. Maung and G. Baskaran [2000], "Diaphragm Wall and Barrette Construction for Thiam Ruam Mit Station Box, MRT Chaloem Ratchamongkhon Line, Bangkok," *Proc. GeoEng2000 – An Intern. Conf. on Geotechnical & Geological Engineering*, Melbourne, Australia, 6 pp.

Tureyen, E.J. and R.J. Frosch [2003], "Concrete Shear Strength: Another Perspective," *ACI Structural Journal*, Vol. 100, No. 5, pp. 609-615.